Received: 8 July 2017 | Revised: 28 November 2017 | Accepted: 12 December 2017

DOI: 10.1002/term.2632

RESEARCH ARTICLE

WILEY

Collagen nanofibre anisotropy induces myotube differentiation and acetylcholine receptor clustering

Frank H. Kung[1] | David Sillitti[2] | Anil B. Shrirao[2] | David I. Shreiber[2,3] | Bonnie L. Firestein[1,3]

[1] Department of Cell Biology and Neuroscience, Rutgers University, Piscataway, NJ, USA

[2] Department of Biomedical Engineering, Rutgers University, Piscataway, NJ, USA

[3] Graduate Faculty in Biomedical Engineering, Rutgers University, Piscataway, NJ, USA

Correspondence
Bonnie L. Firestein, Department of Cell Biology and Neuroscience, Rutgers University, 604 Allison Road, Piscataway, NJ 08854, USA.
Email: firestein@biology.rutgers.edu

Funding information
New Jersey Commission on Spinal Cord Research, Grant/Award Number: CSCR14IRG005

Abstract

To create musculoskeletal tissue scaffolds for functional integration into host tissue, myotubes must be properly aligned with native tissue and spur the formation of neuromuscular junctions. However, our understanding of myoblast differentiation in response to structural alignment is incomplete. To examine how substrate anisotropy mediates myotube differentiation, we studied C2C12 myoblasts grown on aligned collagen substrates in the presence or absence of agrin. Myoblasts grown on microfluidically patterned collagen substrates demonstrated increased multinucleated myotubes and nicotinic acetylcholine receptor (AChR) clusters. However, agrin treatment did not synergistically increase differentiation of myoblasts seeded on these patterned collagen substrates. Myoblasts grown on aligned electrospun collagen nanofibres also demonstrated increased formation of multinucleated myotubes and AChR clusters, and agrin treatment did not increase differentiation of these cells. Using fluorescently labelled collagen nanofibres, we found that AChR clustered in cells grown on nanofibres with significantly higher anisotropy and that this clustering was eliminated with agrin treatment. Interestingly, anisotropy of substrate had no effect on the localization of AChRs along the myotube, suggesting that additional signalling pathways determine the specific location of AChRs along individual myotubes. Taken together, our results suggest a novel role for fibre anisotropy in myotube differentiation, specifically AChR clustering, and that anisotropy may guide differentiation by activating similar pathways to agrin. Our data suggest that agrin treatment is not necessary for differentiation and maturation of myoblasts into myotubes when myoblasts are grown on aligned collagen substrates.

KEYWORDS

muscle differentiation, musculoskeletal tissue engineering, myotube, neuromuscular junction, tissue engineering, topographical cues

1 | INTRODUCTION

There is an increased need for scaffolds for musculoskeletal tissue engineering because these tissues are routinely damaged in sports activities and during almost any surgical procedure (Järvinen & Lehto, 2012). To successfully integrate with host musculoskeletal tissue, scaffolds must meet a variety of requirements. For example, these tissue scaffolds must (a) allow myoblasts to properly differentiate into functional myotubes, (b) properly align with native tissue to repair or replace missing tissue from the patient, and (c) spur the formation of neuromuscular junctions (NMJs) for proper integration with host tissue peripheral nervous tissue. To create successful musculoskeletal tissue scaffolds, a better understanding of how materials and material properties affect myotube differentiation and NMJ formation is needed.

The use of topographical cues, that is, specifically creating aligned scaffolds, has been found to be beneficial for musculoskeletal tissue engineering. Seeding myoblasts on polydimethylsiloxane (PDMS) micropatterns or poly(lactic acid) scaffolds increases the differentiation of myoblasts into myotubes as demonstrated by increased myotube length, myotube striation, and decreased myoblast proliferation (Huang et al., 2006). Recently, a wide variety of electrospun aligned materials, including poly(epsilon-caprolactone)/collagen, poly(lactide-co-glycolide), poly(hydroxybutyrate), and chitosan, have been fabricated for musculoskeletal tissue engineering and have been used to

show that increased differentiation of myoblasts into myotubes occurs on multiple types of substrates (Aviss, Gough, & Downes, 2010; Choi, Lee, Christ, Atala, & Yoo, 2008; Ricotti et al., 2012). Furthermore, the topography of the substrate upon which myotubes are grown affects myoblast differentiation. For example, when myoblasts are grown on micropatterned PDMS substrates containing posts and trenches of various sizes and shapes, these topologies influence differentiation of the myoblasts into myotubes, and this cellular behaviour is explained by a simple geometrical model of myotube orientation (Gingras et al., 2009). Similarly, our group reported that the growth and differentiation of myoblasts in trenches 50 μm wide lead to individual myotube formation and differentiation, whereas growth of myoblasts in smaller or larger trenches causes formation of branching myotubes (Langhammer, Kutzing, Luo, Zahn, & Firestein, 2013; Langhammer, Zahn, & Firestein, 2010).

Despite the promise of alignment for increasing the integration of musculoskeletal tissue constructs with host tissue, research is lacking on identification of the specific molecular signalling pathways activated by topographical cues. Only in the past 3 years has it been demonstrated that alignment of myoblasts causes an upregulation of differentiation factors, such as MyoD, MyoG, and MyHC, and increased expression of important cell adhesion molecules, such as integrin α7β1, in vitro (Jana, Leung, Chang, & Zhang, 2014; McClure et al., 2016). In addition, it was recently demonstrated that myoblasts grown on aligned scaffolds show increased expression of dystrophin in vivo, thus potentially acting as a viable palliative for Duchenne's muscular dystrophy (Yang et al., 2014). These reports demonstrate that the local topography of the substrate on which myoblasts are seeded plays an important role in promoting the differentiation of myoblasts into myotubes, maturation of myotubes, and regulating integration with host tissues.

Although alignment increases the fusion of myoblasts into multinucleated myotubes, the effect of topographical cues upon the formation of nicotinic acetylcholine receptor (AChR) clusters and the formation of functional NMJs is unknown. Moreover, a subset of myotube differentiation factors that is upregulated after alignment plays important roles in the formation of AChR clusters, suggesting that alignment may spur the formation of AChR clusters or functional NMJs. For example, the transcription factor MyoD and adhesion protein integrin α7β1 are upregulated after alignment (McClure et al., 2016) and promote AChR clustering (Burkin, Kim, Gu, & Kaufman, 2000; Dutton, Simon, & Burden, 1993). However, more detailed analyses on how aligned topographical features affect AChR formation have not yet been performed. Understanding how NMJs form in response to aligned topographical features will inform us on how to create scaffolds that better integrate with host tissue.

Here, we investigate how alignment affects AChR clustering in myotubes formed from myoblasts seeded and grown on patterned collagen substrates and on a collagen nanofibre scaffold. Our results are the first to demonstrate that AChR clustering increases in response to substrate alignment, and we show that this increase in clustering likely signals via the same molecular pathway as does agrin to induce AChR clustering. Furthermore, we report that AChR clustering is sensitive to small differences in collagen nanofibre anisotropy. Finally, we find that this anisotropic sensitivity is limited to individual myotubes but does not induce region-specific expression of AChR clustering in myotubes.

2 | METHODS

2.1 | Microfluidic channel fabrication and collagen patterning

Microfluidic devices were fabricated as previously described (Shrirao, Kung, Yip, Cho, & Townes-Anderson, 2014). Briefly, silicon wafers were cleaned with 100% acetone, isopropyl alcohol, and ethanol for 10 min before dehydrating them in an oven (150 °C) overnight. SU-8 2025 (Microchem) was spin-coated onto the silicon wafers at a thickness of 41 μm. SU-8 was baked at 65 °C for 2 min and at 95 °C for 7 min before exposure to 160 mJ/cm^2 ultraviolet (UV) with a mask aligner EVG 620. Post-exposure, silicon wafers were baked at 65 °C for 1 min and at 95 °C for 3 min. Wafers were developed in SU-8 developer for 5 min, washed with 100% isopropyl alcohol, and hard baked overnight in an oven at 150 °C. Silicon masters were then silanized for 1 hr with (tridecafluoro-1,1,2,2-tetrahydrooctyl)-1-trichlorosilane vapours (United Chemical Technology Inc., Levittown, PA, USA) under vacuum. PDMS (Sylgard 184, Dow Corning Inc., USA) elastomer and curing agent were mixed in a 10:1 weight ratio, poured over the top of the silicon masters, degassed for 30 min, and then polymerized in a 65 °C oven for at least 2 hr before being cut out from the silicon wafers. One-millimetre inlets and outlets were punched into each PDMS device and then sterilized with 70% ethyl alcohol, washed 3 times with water, and placed under UV radiation for 30 min prior to use.

Collagen was patterned using the microfluidic devices as previously reported (Shrirao et al., 2014; Shrirao et al., 2017). Briefly, sterilized PDMS microfluidic devices were placed onto cleaned 22-mm square glass coverslips in a 6-well cell culture plate. Collagen type 1 solution (30 μl of 0.01%; Sigma Aldrich, cat#: C8919) was diluted in phosphate-buffered saline (PBS) and placed onto the inlet and outlet of the microfluidic device, and then the device was placed into a vacuum chamber for 10 min. The vacuum was removed, and the entire apparatus was placed into a cell culture incubator overnight. Excess collagen was aspirated from the microfluidic devices, and the device was removed from the glass coverslip and discarded. Glass coverslips were washed 3 times with PBS. Confirmation of collagen patterning was performed by staining with 50 μM N-Hydroxysuccinimide (NHS)-fluorescein (5/6-carboxyfluorescein succinimidyl ester) mixed isomer (Thermo-Fisher, cat#: 46409) for 1 hr and then subsequently washing 3 times with PBS, mounting the 22-mm square coverslips with Fluoromount G (Southern Biotech, cat# 0100-01), and imaging on an EVOS® FL microscope (Thermo-Fisher, Cat#: AMF4300) at 40× magnification. Patterned and unpatterned coverslips to be used for cell culture were coated overnight with a 1% bovine serum albumin solution in PBS. Patterned glass coverslips were washed 3 times with PBS and used for subsequent experiments.

2.2 | Production and characterization of electrospun collagen nanofibres

Solutions of 8 wt% lyophilized collagen (Bovine type I, Kensey Nash, Exton, PA, USA) were prepared in 1,1,1,3,3,3-hexafluoro-2-propanol (Oakwood Chemical, Estill, SC, USA) (Boland et al., 2004) for 24 hr. Electrospinning was performed onto either a grounded metal plate or a grounded rotating metal drum, 17 cm from the needle tip, at speeds of 865 m/min at the drum surface. Electrospinning solution was ejected at 0.25 ml/hr with an accelerating voltage of 15 kV. Scanning electron microscopy images (i.e., as shown in Figure 1) were prepared and analysed using a Zeiss Sigma field emission scanning electron microscope.

2.3 | Fluorescent labelling of collagen nanofibres

Collagen nanofibres were fluorescently labelled using Alexa Fluor™ 555 NHS ester (succinimidyl ester; Thermo Fisher, cat# A37571). Collagen nanofibres were sterilized with UV irradiation for 30 min. Collagen nanofibres were then labelled with 50 μM Alexa Fluor™ 555 NHS ester (succinimidyl ester) dissolved in 0.5% dimethyl sulfoxide and PBS. Plates were protected from ambient light and placed onto a shaker for 1 hr. Collagen nanofibres were then washed 3 times with PBS before seeding with C2C12 myoblasts as described below.

2.4 | Cell growth and maintenance

C2C12 mouse myoblast cells (American Type Culture Collection, Manassas, VA, USA) were grown in T75 flasks in growth medium (Dulbecco's modified Eagle's medium + 10% fetal bovine serum). Only cultures below Passage 15 were used. At ~70% confluency, myoblasts were trypsinized and diluted to 500,000 cells per patterned coverslip or 200,000 cells per well for coverslips with or without nanofibre mats or random and aligned collagen nanofibres. At day in vitro (DIV) 2, growth medium was aspirated from each well and replaced with differentiation medium (Dulbecco's modified Eagle's medium + 2% horse serum). At DIV7, cells on mats were fixed with 4% paraformaldehyde in PBS and immunostained with rabbit anti-desmin (1:500; Sigma Aldrich, cat# D1033), α-bungarotoxin Alexa Fluor® 488 conjugate (Thermo-Fisher, cat# B13422), and Hoechst 33225. Myotubes were imaged at 200× with an EVOS® FL microscope (Thermo-Fisher, cat# AMF4300). Myotube formation was evaluated by manual counting of a number of multinucleated cells, cell nuclei, number of AChR clusters, and AChR cluster size.

2.5 | Analysis of nanofibre anisotropy

Nanofibre isotropy was analysed using a modified version of the FibrilJ plugin developed by Sokolov, Belousov, Bondarev, Zhouravleva, and Kasyanenko (2017). Briefly, fluorescently labelled nanofibres were imaged at 200× with an EVOS® FL microscope. Labelled images were divided into 50 pixel × 50 pixel segments, and each segment was evaluated for anisotropy using the FibrilJ plugin (i.e., as shown in Figure 4). To correlate myotube growth and differentiation with nanofibre anisotropy, regions of nanofibres with differentiated myotubes were segmented into 50 pixel × 50 pixel segments and evaluated by FibrilJ for anisotropy and fibre orientation (i.e., as shown in Figure 4).

2.6 | Statistical analysis

One-way analysis of variance followed by the appropriate multiple comparisons test was performed using GraphPad Prism 7.0 (GraphPad, La Jolla, CA, USA). A p value <.05 was considered significant.

3 | RESULTS

3.1 | PDMS patterning and collagen nanofibre fabrication

To examine how myoblast geometry affects myotube differentiation and clustering of nicotinic AChRs, PDMS microfluidic patterning of collagen substrates or aligned collagen nanofibre scaffolds was used. Patterned collagen substrates were fabricated as previously described utilizing vacuum-assisted patterning (Shrirao et al., 2014; Shrirao et al., 2017). Microfluidic devices used for this experiment contained channels of 10 μm width, which are separated by walls of 200 μm thickness, creating patterned collagen. Collagen patterning on glass coverslips was confirmed via staining with NHS-fluorescein (5/6-carboxyfluorescein succinimidyl ester; Figure 1a–c). Each microfluidic channel created similar patterns of single lanes of collagen substrate ~10 μm in width. For nanofibres, collagen was electrospun in both random and aligned formats (Figure 1d,e). Collagen nanofibres were fabricated from a solution of collagen in hexafluoroisopropanol by electrospinning the fibres onto aluminium foil attached to either a flat grounding plate (random fibres) or a high-speed rotating mandrel as the grounding mechanism (aligned fibres; Aviss et al., 2010; Choi et al., 2008). Alignment of collagen nanofibres was confirmed via scanning electron microscopy (Figure 1b).

3.2 | Effects of patterned collagen and agrin on differentiation of myotubes and clustering of AChRs are not additive

To determine the effect of collagen substrate alignment on myotube differentiation and AChR cluster formation, unpatterned and patterned collagen substrates (fabricated by microfluidic patterning methods as previously described; Shrirao et al., 2014; Shrirao et al., 2017) were seeded with C2C12 myoblasts, and the myoblasts were differentiated into myotubes via serum deprivation after DIV2. After fixation, the cells were stained for nuclei and AChR clusters with Hoechst 3352 and α-bungarotoxin conjugated to Alexa Fluor 488, respectively. Multinucleated myotubes could be clearly distinguished from surrounding undifferentiated cells (Figure 2a). To control for initial cell number in each condition, individual nuclei were counted in each image and normalized to unpatterned collagen in each experiment. No statistically significant differences in the number of nuclei were observed, indicating that cell adhesion and growth do not differ between conditions. The addition of agrin to cell differentiation medium did not affect the number of nuclei (Figure 2b).

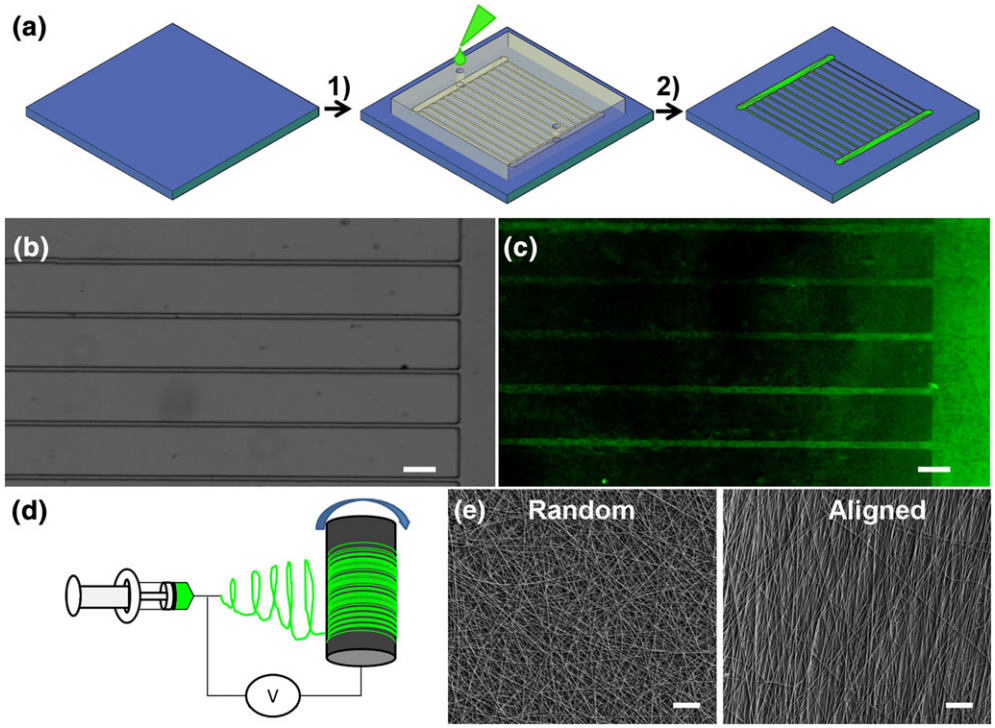

FIGURE 1 Polydimethylsiloxane (PDMS) patterning and electrospinning set-up. (a) Glass coverslips were patterned using vacuum-assisted PDMS microfluidic devices as follows: (1) Microfluidic devices were placed onto clean 22-mm glass coverslips, and 20 μl of droplet of 0.01% collagen solution was injected into the microfluidic channels using the vacuum-assisted protein patterning technique. (2) After incubation at 37 °C for 24 hr, PDMS microfluidic devices were removed from the coverslip and coated with 2% bovine serum albumin in phosphate-buffered saline solution for another 24 hr prior to seeding with C2C12 myoblasts. (b) Microfluidic device. Microfluidic device contained channels 10 μm in width separated by 200 μm. Scale bar = 100 μm. (c) Collagen patterned by microfluidic device. Collagen was stained with NHS-succinylmide-ester fluorescein. Collagen patterning was confirmed by fluorescent imaging. Scale bar = 100 μm. (d) Electrospinning set-up. Collagen solution was electrospun onto a high-speed rotating mandrel to align collagen fibres. A high-voltage power source was attached to a syringe pump and to the metal mandrel. The syringe was placed onto the pump, which slowly injected solution into the high-voltage environment, causing collagen nanofibres to adhere to the rotating metal mandrel to align the collagen nanofibres. (e) Scanning electron microscopy of electrospun collagen nanofibres. Random nanofibres were electrospun onto a grounded metal plate, whereas aligned nanofibres were spun onto a grounded rotating metal mandrel. Scale bars = 10 μm

We then quantitated the number of individual multinucleated myotubes, as identified by staining with Hoechst 3352 and α-bungarotoxin conjugated to Alexa Fluor 488. AChR clusters were distinguishable from background staining, allowing for identification of individual myotubes (Figure 2a). Growth on aligned collagen increased the number of multinucleated myotubes when normalized to those grown on unpatterned collagen (Figure 2b), suggesting that alignment promotes differentiation. In contrast to what we expected (Barik, Zhang, Sohal, Xiong, & Mei, 2014; Bezakova & Ruegg, 2003; Martin & Sanes, 1997; Trinidad, Fischbach, & Cohen, 2000; Weston, Teressa, Weeks, & Prives, 2007), the addition of agrin to the medium did not increase the number of multinucleated myotubes on the aligned collagen samples, suggesting that agrin treatment may occlude the effect of patterned collagen on differentiation. In unpatterned collagen samples, agrin significantly increased the number of multinucleated myotubes, confirming its activity and consistent with previous work (Aviss et al., 2010; Choi et al., 2008; Gingras et al., 2009; Yang et al., 2014).

Because AChR clustering serves as a marker for myotube maturity and is crucial for the proper development of NMJs (Menon, Carrillo, & Zinn, 2013; Tintignac, Brenner, & Rüegg, 2015), we examined the formation of AChR clusters when cells were grown on unpatterned and aligned collagen in the absence or presence of agrin. We quantitated the total number of AChR clusters divided by total number of multinucleated myotubes in each image and normalized to this metric to that of cells grown on unpatterned collagen. Collagen alignment or agrin addition to the medium significantly increased the number of AChR clusters per myotube (Figure 2b). However, when cells were grown on aligned collagen and simultaneously treated with agrin, the effect of the individual treatments was not additive, suggesting a shared mechanism between the two treatments or a maximum threshold of AChR clustering (Figure 2b). Furthermore, the average area of each AChR cluster increased in response to agrin regardless of collagen patterning, although collagen alignment alone had no effect (Figure 2b). Taken together, these data suggest that the size of AChR clusters may be controlled by a molecular pathway activated specifically by agrin but not by alignment.

3.3 | Collagen nanofibres and agrin treatment promote myotube differentiation and AChR clustering

Because the micropatterned collagen substrate on the glass slides is not a biologically relevant system for tissue engineering, we constructed collagen nanofibres and seeded and differentiated myoblasts on these fibres. C2C12 myoblasts were seeded on random and aligned

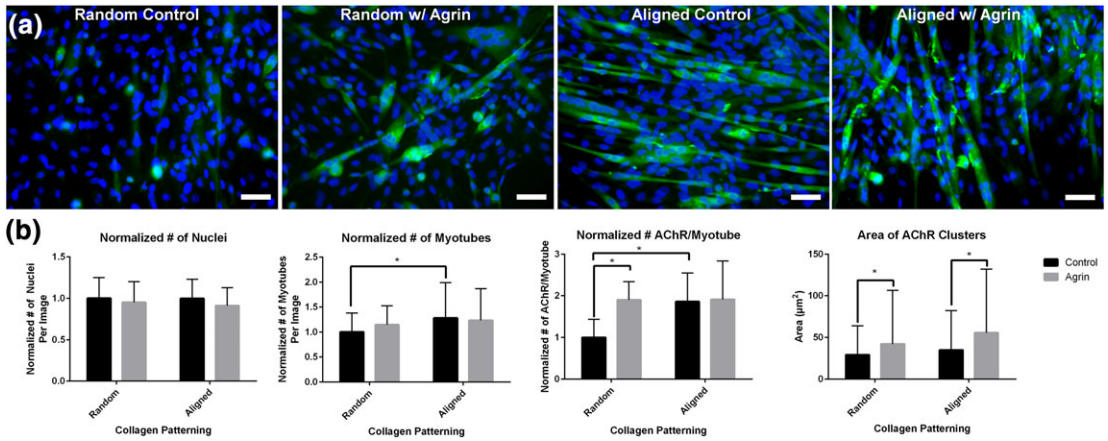

FIGURE 2 Differentiation of myotubes and clustering of acetylcholine receptors (AChRs) by collagen patterned by polydimethylsiloxane and agrin are not additive. (a) Example myotubes formed on random or aligned patterns of collagen on glass coverslips in the absence or presence of agrin. From left to right: C2C12 cells plated onto randomly aligned collagen patterns, C2C12 cells plated on aligned nanofibres, C2C12 cells plated onto randomly aligned collagen patterns and treated with agrin, and C2C12 cells plated on aligned collagen patterns and treated with agrin. Scale bars = 50 μm. Myotubes were stained for AChRs (green) and nuclei (blue) with α-bungarotoxin Alexa Fluor 488 and Hoechst 35288, respectively. (b) Differentiation of myotubes and clustering of AChRs in the four different conditions. Nuclei were counted in each image by staining with Hoechst 35288, thresholding in ImageJ, and utilizing the particle analysis plugin. Number of multinucleated myotubes was examined by analysing AChR staining with α-bungarotoxin Alexa Fluor 488 and determining the presence of multiple nuclei in each cell. AChR clusters were counted in each image and divided by the total number of myotubes per image. Quantification of differentiation was normalized to myotubes grown on randomly patterned collagen. No significant increase in the number of myotubes was seen in cultures grown on aligned collagen whether or not agrin was present. Error bars = standard deviation. n = 4 cultures, 60 images per culture. $^*p < .05$ determined by one-way analysis of variance and Tukey's post hoc analysis

collagen nanofibres and differentiated by serum deprivation into myotubes (Figure 3a). Cultures were fixed and stained for nuclei and AChRs, and similar to the analysis of cells grown on patterned collagen substrates, multinucleated myotubes and AChR clusters were quantified and normalized to those present on random nanofibres (Figure 3a).

We observed that significantly fewer nuclei were present on aligned collagen nanofibres than were present on the random collagen nanofibres (Figure 3b). Interestingly, despite the fact that fewer nuclei were present, the number of multinucleated myotubes was greater when cells were grown on aligned collagen samples in the absence or

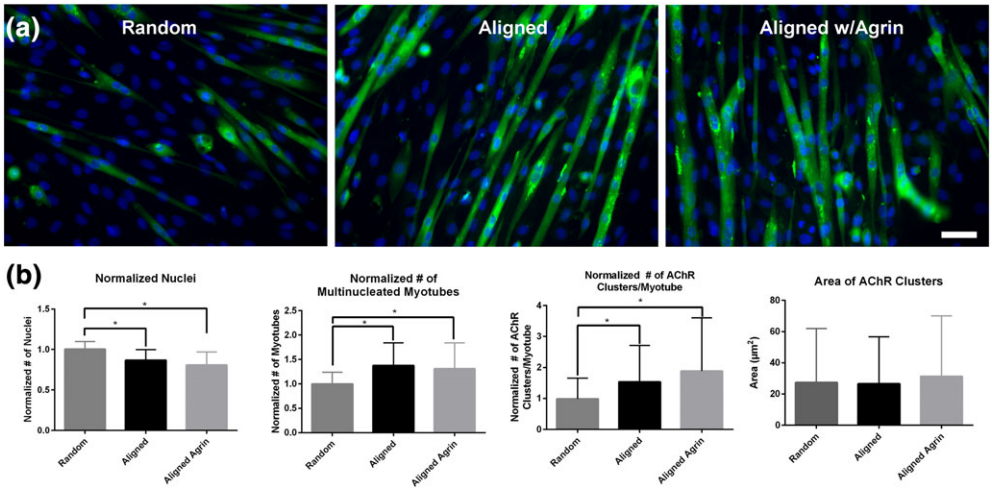

FIGURE 3 Differentiation of myotubes and acetylcholine receptor (AChR) clustering are enhanced by collagen nanofibre alignment and agrin in a nonadditive manner. (a) Example myotubes that form on collagen electrospun nanofibres. From left to right: Myotubes grown on randomly electrospun nanofibres, myotubes grown on aligned nanofibres, and myotubes grown on aligned nanofibres and treated with agrin. Myotubes are stained for AChR and nuclei with α-bungarotoxin Alexa Fluor 488 (green) and Hoechst 35288 (blue), respectively. Scale bar = 50 μm. (b) Quantitation of myotube differentiation and AChR formation in conditions shown in panel (a). Nuclei were counted in each image by staining with Hoechst 35288, thresholding in ImageJ, and utilizing the particle analysis plugin. Number of multinucleated myotubes was examined by analysing AChR staining with α-bungarotoxin Alexa Fluor 488 and examining the presence of multiple nuclei in each cell. AChR clusters were counted in each image and divided by the total number of myotubes per image. Quantification of differentiation was normalized to that of myotubes grown on randomly electrospun nanofibres in the absence of agrin. Error bars = standard deviation. n = 4 cultures, 60 images per culture. $^*p < .05$ determined by one-way analysis of variance and Tukey's post hoc analysis

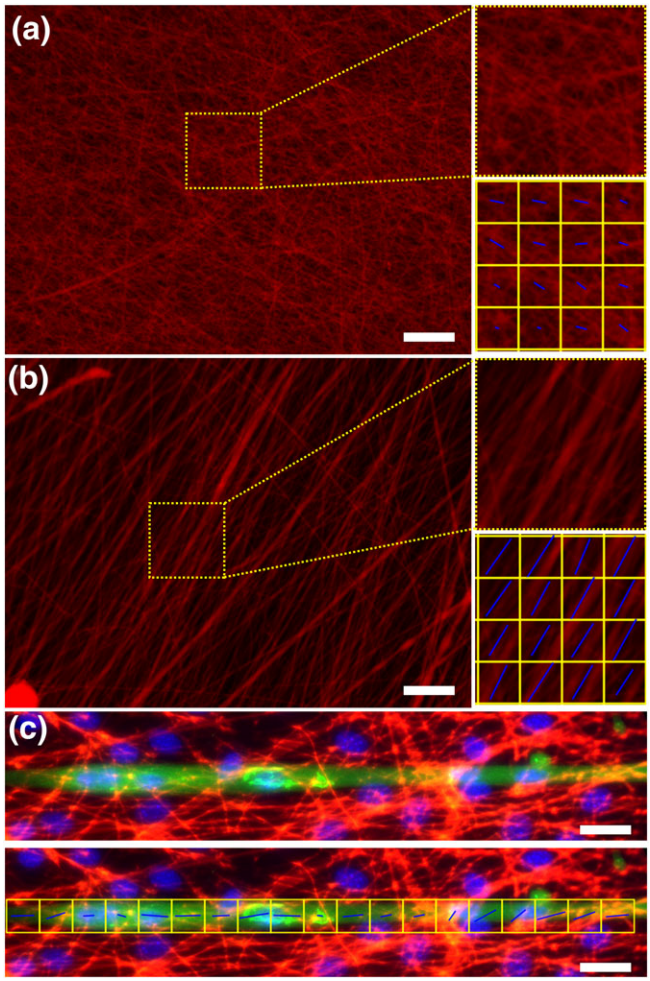

FIGURE 4 Example of measurement of collagen nanofibre alignment. Collagen nanofibres were fluorescently labelled with Alexa Fluor™ 555 NHS ester (succinimidyl ester), allowing for live monitoring using fluorescent microscopy. Alignment of collagen nanofibres was analysed via FibrilJ by image segmentation. The lengths of blue lines indicate the level of anisotropy measured from each yellow region of interest. Orientation of blue lines indicates average fibril orientation for the particular segment. (a) Anisotropy analysis of random electrospun collagen nanofibres. Scale bar = 50 μm. (b) Anisotropy analysis of aligned collagen nanofibres. Scale bar = 50 μm. (c) Anisotropy analysis of collagen nanofibres underlying individual myotubes stained for acetylcholine receptor and nuclei with α-bungarotoxin 488 and Hoechst 35288, respectively. Scale bars = 25 μm

presence of agrin (Figure 3b), indicating an increase in differentiation from myoblasts to myotubes. Treatment with agrin alone promoted the same changes to nuclei and number of myotubes; however, treatment of cells grown on aligned nanofibres with agrin resulted in the same degree of differentiation of myoblasts to myotubes that resulted from either condition alone. These data further suggest a shared mechanism between alignment and agrin in promoting differentiation.

Because patterned collagen substrate increases AChR clustering in multinucleated myotubes, we asked whether aligned substrates promote AChR cluster formation. We quantitated AChR clusters by dividing total number of multinucleated myotubes per image and normalizing to this metric from cells grown on random collagen nanofibres and found that the number of AChR clusters per myotube increased in cultures grown on aligned collagen myotubes whether or not the cultures were treated with agrin (Figure 3b), suggesting a shared mechanism between the two treatments or a maximum threshold of AChR clustering. In contrast to what we observed when cultures were grown on patterned collagen, the size of AChR clusters did not significantly differ in any experimental condition, suggesting that collagen nanofibre alignment and agrin treatment do not enhance AChR cluster size under these experimental conditions (Figure 3b).

3.4 | Collagen nanofibre anisotropy changes after cultured with C2C12 cells for 2 days

Because it is possible that growth and differentiation of myoblasts can remodel the collagen nanofibres on which they are grown, we examined the structure of electrospun collagen nanofibres during differentiation of myoblasts or in response to factors secreted by the cells. Collagen nanofibres were fluorescently labelled with either NHS-fluorescein (5/6-carboxyfluorescein succinimidyl ester) or Alexa Fluor™ 555 NHS ester (succinimidyl ester), allowing for live monitoring of collagen nanofibre structure using fluorescent microscopy (Figure 4). Growth and differentiation of myoblasts had no effect on the anisotropy of random fibres; however, myoblast growth decreased the anisotropy of aligned fibres over the 2-day post-seeding, and this decrease was observed regardless of whether agrin was present (Figure 5a,b). These data suggest that myoblast growth and differentiation may act to remodel the surrounding substrate.

3.5 | Myotube differentiation correlates with fibre anisotropy

Because C2C12 cells alter collagen nanofibre anisotropy (Figure 5a,b), we determined how collagen nanofibre anisotropy affects the expression of and the localization of AChR clusters by dividing each myotube into even regions and measuring collagen nanofibre anisotropy of those regions using a modified version of FibrilJ ImageJ plugin. In addition, we quantified total nanofibre density by measuring the fluorescent intensity of each region fluorescing Alexa Fluor™ 555 NHS ester. For all quantifications, measurements were normalized to those of myotubes on random collagen nanofibres. In myotubes seeded on randomly electrospun collagen nanofibres, myotubes with AChR clusters occurred less frequently on nanofibres with higher anisotropy (Figure 6a,b). However, in myotubes seeded on aligned electrospun collagen nanofibres, myotubes with AChR clusters formed on nanofibres with high levels of anisotropy more frequently than did those without AChR clusters (Figure 6b). This difference in myotube preference for fibre anisotropy did not occur in myotubes on aligned nanofibres that were treated with agrin. Furthermore, myotubes containing AChR clusters only grow on higher nanofibre density when grown on random nanofibres. These data suggest that myotube fusion results from different mechanisms when myoblasts are seeded on random collagen nanofibres versus aligned nanofibres.

As cellular events are often regulated by the local environment, we examined if local collagen nanofibre anisotropy correlates with the

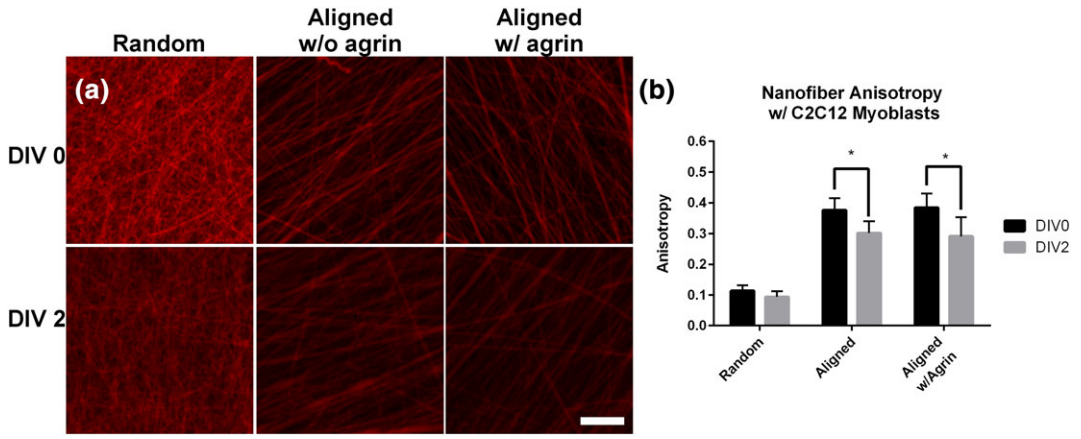

FIGURE 5 Collagen nanofibre anisotropy decreases after cultured with C2C12 cells for 2 days. (a) Example nanofibres fluorescently labelled with NHS-ester Alexa Fluor 555. Top row: Two sets of fibres on day in vitro (DIV) 0. Bottom row: Two sets of fibres on DIV2. Left: Randomly aligned nanofibres seeded with C2C12 myoblasts. Centre: Aligned nanofibres seeded with C2C12 myoblasts. Right: Aligned nanofibres seeded with C2C12 myoblasts and treated with agrin. Scale bars = 50 μm. (b) Anisotropy measurements of fibres seeded with C2C12 myoblasts in panel (a). Error bars = standard deviation. n = 4 cultures, 5 images per time point per culture. *p < .05 as determined by one-way analysis of variance and Tukey's post hoc analysis

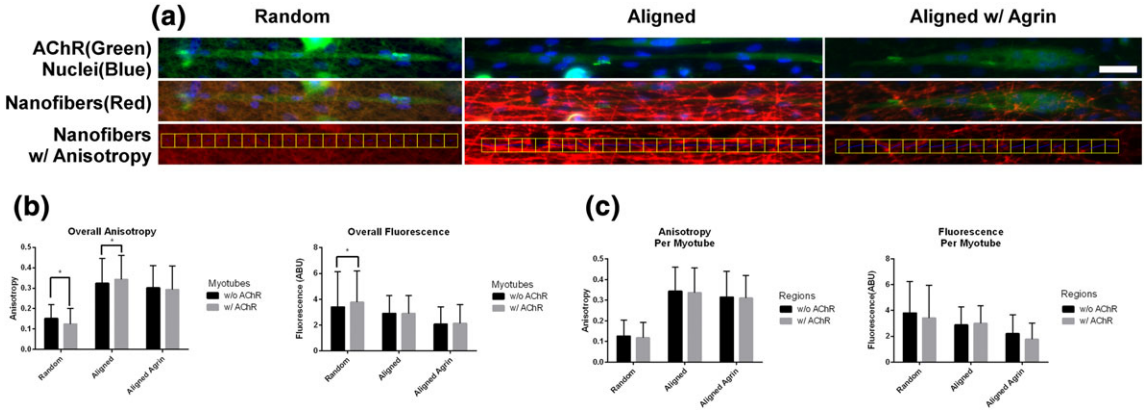

FIGURE 6 Myotube differentiation correlates with fibre anisotropy. (a) Example myotubes grown on fluorescently labelled collagen nanofibres. Acetylcholine receptor (AChR) clusters identified via staining with α-bungarotoxin 488 after growth and differentiation on labelled collagen nanofibres. Nanofibres were then imaged, and their structure was evaluated using FibriIJ anisotropy analysis. Scale bar = 50 μm. (b) On average, myotubes containing AChR clusters prefer to grow on collagen nanofibres with higher levels of anisotropy than do myotubes without AChR clusters. This effect is attenuated with agrin treatment. Individual myotubes with higher levels of AChR clusters have no preference for growth on fibres with higher anisotropy. No significant difference in overall collagen nanofibre fluorescence was found in myotubes either without AChR clusters or with AChR clusters on aligned nanofibres or aligned nanofibres with agrin containing differentiation medium. No significant difference in overall collagen nanofibre fluorescence was found on aligned nanofibres or aligned nanofibres with agrin containing differentiation medium. Error bars = standard deviation. n = 4 cultures, 60 images per culture. *p < .05 determined by one-way analysis of variance and Tukey's post hoc analysis. ABU = arbitrary units. (c) Specific regions of myotubes with and without AChR clusters do not show a preference for aligned nanofibres. No significant difference was found between fluorescence per myotube for cells on aligned nanofibres versus cells on aligned nanofibres plus agrin treatment. Error bars = standard deviation. *p < .05 determined by one-way analysis of variance and Tukey's post hoc analysis. n = 4 cultures, 60 images per culture. ABU = arbitrary units

localization of AChR cluster formation. Collagen nanofibre anisotropy was compared in regions of myotubes with AChR clusters or without AChR clusters (Figure 6a). In these regions, no correlation was found for cells grown on random electrospun nanofibres, aligned nanofibres, or aligned nanofibres in the presence of agrin. These data suggest that although the structure of collagen nanofibres may preferentially increase the expression of AChR clusters in individual myotubes, these differences in structural anisotropy in collagen nanofibres do not promote local clustering of AChR in myotubes. Additionally, the addition of agrin did not promote local effects of nanofibre anisotropy (Figure 6b). As a control, we determined the amount of nanofibres on which myotubes with and without AChR clusters grew and determined that in each condition, both classes of myotubes covered similar density of nanofibres as determined by fluorescence of fibres (Figure 6c). Taken together, this analysis suggests that in this setting, the amount of collagen nanofibre on which myotubes are grown plays a less important role in AChR cluster formation than collagen nanofibre structural anisotropy.

4 | DISCUSSION

4.1 | Topographical alignment and agrin share similar myotube differentiation pathways

In our study, we demonstrated that topographical cues increase both myotube differentiation and the formation of AChR clusters. We found that this increase in myotube differentiation occurs when myoblasts are plated on either aligned collagen substrates on glass coverslips or electrospun aligned collagen nanofibres. Specifically, our data are the first to examine how cell substrate topography affects the formation of AChR clusters and supplies evidence that alignment- and agrin-promoted AChR clustering shares a common signalling mechanism. Our work suggests that this specific topographically sensitive signalling pathway may interact with other pathways utilized by myotubes to form AChR clusters and subsequently NMJs. In specific, we demonstrate the lack of additional myotube differentiation and AChR formation when alignment and agrin are applied together to differentiating myotubes. We believe that this is the first report demonstrating that AChR clustering increases in response to substrate alignment.

Previous work demonstrated that alignment leads to the upregulation of the integrin receptor α7β1 and that this receptor is a crucial component of the differentiation pathway during myotube alignment (McClure et al., 2016; Zhang, Sun, Lee, Abdeen, & Kilian, 2016). Additionally, integrin receptor α7β1 specifically activates the myotube transcription factor MyoD (McClure et al., 2016; Zhang et al., 2016), which is vital for proper formation of both multinucleated myotubes and AChR cluster formation (Piette, Bessereau, Huchet, & Changeux, 1990; Rudnicki & Jaenisch, 1995; Weintraub, 1993). From our study, we propose a model of myotube differentiation and interaction between alignment and agrin that demonstrates how alignment and agrin can interact along the same pathways and thus not increase AChR formation in aligned samples (Figure 7).

In this model, aligned substrates increase the expression of integrin α1β7 (McClure et al., 2016), and downstream signalling is key to inducing agrin-related AChR clustering (Bezakova & Ruegg, 2003; Burkin et al., 2000; Martin & Sanes, 1997). Alignment increases integrin signalling and may subsequently begin a cascade of signalling, leading to an eventual downregulation of the late differentiation factor paired box protein (PAX7) and upregulation of late differentiation factor MyoD (McClure et al., 2016). The addition of agrin to myoblast cell cultures leads to additional AChR formation via the MyoD pathway (Anderson & Grow, 2012) but not in myoblast cultures where MyoD is already activated by topographical alignment.

Our work suggests that other molecules may be necessary to increase AChR cluster formation in myoblasts grown on aligned substrates. We speculate that these molecules include laminin (Burkin et al., 2000; Weston et al., 2007), WNT3 (Barik et al., 2014; Henriquez et al., 2008; Korkut & Budnik, 2009), and neuregulin (Buonanno & Fischbach, 2001; Trinidad et al., 2000), which co-stimulate AChR formation over AChR formation by agrin alone. Therefore, it may be necessary to use co-stimulators, such as the ones listed above or others, to induce further AChR cluster formation in developing myoblasts and to create functional NMJ for musculoskeletal tissue-engineered constructs.

In addition, future studies will determine the level of anisotropy necessary to activate these signalling pathways and determine if different levels of anisotropy affect the response to these co-stimulatory molecules. Other than comparing patterned and unpatterned conditions, our study did not determine the levels of anisotropy needed to affect AChR clustering or how anisotrophy affects the response to co-stimulatory molecules.

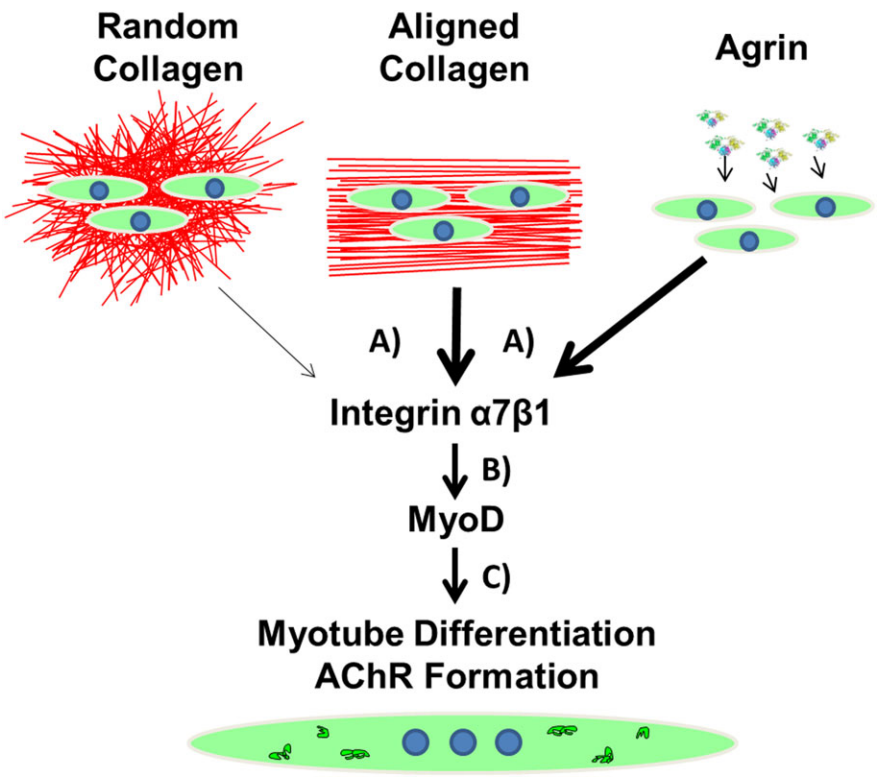

FIGURE 7 Proposed model for myotube differentiation and acetylcholine receptor (AChR) clustering promoted by collagen alignment and agrin. (A) Aligned collagen nanofibres and agrin both activate integrin α7β1 receptors (Burkin et al., 2000; Martin & Sanes, 1997; McClure et al., 2016; Zhang et al., 2016), (B) which in turn activate MyoD (McClure et al., 2016; Zhang et al., 2016). (C) MyoD subsequently increases myoblast differentiation and myotube formation (Anderson & Grow, 2012; Piette et al., 1990; Rudnicki & Jaenisch, 1995; Weintraub, 1993). MyoD then acts to increase AChR clustering in differentiated myotubes (Anderson & Grow, 2012; Piette et al., 1990; Rudnicki & Jaenisch, 1995; Weintraub, 1993)

4.2 | Topographical cues affect levels of AChR clustering but not localization in individual myotubes

Our study demonstrates that individual myotubes are sensitive to collagen nanofibre structure and that increases in nanofibre anisotropy upregulate the expression of AChR clusters within individual myotubes. Furthermore, this sensitivity to anisotropy is abrogated when agrin is applied to the collagen myotubes, further providing evidence that the signalling pathways that induce AChR clustering by alignment are shared with those activated by agrin.

Despite the finding that AChR clustering in individual myotubes is sensitive to collagen nanofibre anisotropy, we did not find evidence of collagen nanofibre structure anisotropy affecting AChR cluster localization along the myotube. This suggests that although alignment may increase expression of integrin receptors and other myotube differentiating factors, the proteins that are important in determining the final localization of AChRs along a myotube are not sensitive to alignment. These factors may include extracellular receptors or cell adhesion molecules, such as Low-density lipoprotein receptor-related protein 4 (LRP4) (Barik et al., 2014) and neural cell adhesion molecules (NCAMs) (Covault & Sanes, 1986), or cytoskeletal associated proteins, such as muscle-specific kinase (MuSK) (Hubbard & Gnanasambandan, 2013; Trinidad et al., 2000), dystroglycan, and isoforms of protein kinase C (PKC) (Lanuza et al., 2014), all of which are important in the final formation and stabilization of NMJ at specific sites in the myotube.

The ability to control region-specific expression of AChR clusters in scaffolds may be important to specifically guide regenerating peripheral neurons to regions of the myotube where AChRs are developing and clustering. Doing so may increase the number of functional NMJs in the tissue-engineered construct and increase functionality. From our study, it appears that altering the topography of a scaffold is not sufficient to enhance AChR formation to a specific region of myotube or scaffold. Our results suggest that alternative strategies, such as spatially specific stimulation with AChR clustering molecules, are necessary for designing constructs with topographically localized AChR clusters. For example, microfluidics have been used to specifically control the regions of myotubes exposed to extracellular agrin and, hence, induce AChR cluster formation in areas with greater local concentrations of agrin (Tourovskaia, Kosar, & Folch, 2006; Tourovskaia, Li, & Folch, 2008). Thus, scaffolds may require specific regions primed with stimulatory molecules (Whitehead & Sundararaghavan, 2014) to enhance expression of AChR clusters in specific regions.

4.3 | AChR cluster size in patterned collagen and in collagen nanofibres

AChR cluster size is significantly increased in the presence of agrin when myoblasts are differentiated into myotubes on either random or aligned collagen on glass coverslip; however, cluster size does not significantly increase in the presence of agrin in myoblasts grown on collagen nanofibre scaffolds. It is possible that collagen substrates coated on glass slides may not activate signalling pathways that regulate cluster size that are activated in myoblasts grown on collagen nanofibre scaffolds. It was previously shown that agrin-induced signalling plays a role in initial and long-term clustering of AChRs and that cluster size is dependent upon this long-term signalling (Bezakova & Ruegg, 2003). In addition to agrin, other factors, such as Src, Fyn, Yes, rapsyn, and calpain, play important roles in stabilization of AChR clusters (Chen et al., 2007; Smith, Mittaud, Prescott, Fuhrer, & Burden, 2001), and whether or not these factors are activated in the presence of collagen nanofibres is currently unknown. Identification of the effector pathways stimulated by collagen nanofibres is the subject of future study.

ACKNOWLEDGEMENTS

This work was funded by New Jersey Commission on Spinal Cord Research Grant CSCR14IRG005 (to B. L. F.). We would like to thank Dr. Jeffrey D. Zahn (Rutgers University) for the gracious use of the BioMEMS facility.

CONFLICT OF INTEREST

The authors have declared that there is no conflict of interest.

ORCID

Bonnie L. Firestein http://orcid.org/0000-0002-1679-3565

REFERENCES

Anderson, E. E., & Grow, W. A. (2012). MyoD and Myogenin are required for agrin-induced AChR clustering. *The FASEB Journal*, *26*(1 Supplement), 919.912.

Aviss, K., Gough, J., & Downes, S. (2010). Aligned electrospun polymer fibres for skeletal muscle regeneration. *European Cells & Materials*, *19*, 193–204.

Barik, A., Zhang, B., Sohal, G. S., Xiong, W. C., & Mei, L. (2014). Crosstalk between agrin and Wnt signaling pathways in development of vertebrate neuromuscular junction. *Developmental Neurobiology*, *74*(8), 828–838.

Bezakova, G., & Ruegg, M. A. (2003). New insights into the roles of agrin. *Nature Reviews Molecular Cell Biology*, *4*(4), 295–309.

Boland, E. D., Matthews, J. A., Pawlowski, K. J., Simpson, D. G., Wnek, G. E., & Bowlin, G. L. (2004). Electrospinning collagen and elastin: Preliminary vascular tissue engineering. *Frontiers in Bioscience*, *9*(1422), e32.

Buonanno, A., & Fischbach, G. D. (2001). Neuregulin and ErbB receptor signaling pathways in the nervous system. *Current Opinion in Neurobiology*, *11*(3), 287–296.

Burkin, D. J., Kim, J. E., Gu, M., & Kaufman, S. J. (2000). Laminin and alpha7beta1 integrin regulate agrin-induced clustering of acetylcholine receptors. *Journal of Cell Science*, *113*(16), 2877–2886.

Chen, F., Qian, L., Yang, Z.-H., Huang, Y., Ngo, S. T., Ruan, N.-J., … Ding, Y.-Q. (2007). Rapsyn interaction with calpain stabilizes AChR clusters at the neuromuscular junction. *Neuron*, *55*(2), 247–260.

Choi, J. S., Lee, S. J., Christ, G. J., Atala, A., & Yoo, J. J. (2008). The influence of electrospun aligned poly(epsilon-caprolactone)/collagen nanofiber meshes on the formation of self-aligned skeletal muscle myotubes. *Biomaterials*, *29*(19), 2899–2906.

Covault, J., & Sanes, J. R. (1986). Distribution of N-CAM in synaptic and extrasynaptic portions of developing and adult skeletal muscle. *The Journal of Cell Biology*, *102*(3), 716–730.

Dutton, E. K., Simon, A. M., & Burden, S. J. (1993). Electrical activity-dependent regulation of the acetylcholine receptor delta-subunit gene, MyoD, and myogenin in primary myotubes. *Proceedings of the National Academy of Sciences*, *90*(5), 2040–2044.

Gingras, J., Rioux, R. M., Cuvelier, D., Geisse, N. A., Lichtman, J. W., Whitesides, G. M., … Sanes, J. R. (2009). Controlling the orientation and synaptic differentiation of myotubes with micropatterned

substrates. *Biophysical Journal*, *97*(10), 2771–2779. https://doi.org/10.1016/j.bpj.2009.08.038.

Henriquez, J. P., Webb, A., Bence, M., Bildsoe, H., Sahores, M., Hughes, S. M., & Salinas, P. C. (2008). Wnt signaling promotes AChR aggregation at the neuromuscular synapse in collaboration with agrin. *Proceedings of the National Academy of Sciences of the United States of America*, *105*(48), 18812–18817. https://doi.org/10.1073/pnas.0806300105.

Huang, N. F., Patel, S., Thakar, R. G., Wu, J., Hsiao, B. S., Chu, B., … Li, S. (2006). Myotube assembly on nanofibrous and micropatterned polymers. *Nano Letters*, *6*(3), 537–542.

Hubbard, S. R., & Gnanasambandan, K. (2013). Structure and activation of MuSK, a receptor tyrosine kinase central to neuromuscular junction formation. *Biochimica et Biophysica Acta (BBA) - Proteins and Proteomics*, *1834*(10), 2166–2169. https://doi.org/10.1016/j.bbapap.2013.02.034.

Jana, S., Leung, M., Chang, J., & Zhang, M. (2014). Effect of nano- and micro-scale topological features on alignment of muscle cells and commitment of myogenic differentiation. *Biofabrication*, *6*(3), 035012.

Järvinen, M. J., & Lehto, M. U. K. (2012). The effects of early mobilisation and immobilisation on the healing process following muscle injuries. *Sports Medicine*, *15*(2), 78–89. https://doi.org/10.2165/00007256-199315020-00002.

Korkut, C., & Budnik, V. (2009). WNTs tune up the neuromuscular junction. *Nature Reviews Neuroscience*, *10*(9), 627–634.

Langhammer, C. G., Kutzing, M. K., Luo, V., Zahn, J. D., & Firestein, B. L. (2013). A topographically modified substrate-embedded MEA for directed myotube formation at electrode contact sites. *Annals of Biomedical Engineering*, *41*(2), 408–420. https://doi.org/10.1007/s10439-012-0647-8.

Langhammer, C. G., Zahn, J. D., & Firestein, B. L. (2010). Identification and quantification of skeletal myotube contraction and association in vitro by video microscopy. *Cytoskeleton*, *67*(7), 413–424. https://doi.org/10.1002/cm.20457.

Lanuza, M. A., Santafe, M. M., Garcia, N., Besalduch, N., Tomàs, M., Obis, T., … Tomàs, J. (2014). Protein kinase C isoforms at the neuromuscular junction: Localization and specific roles in neurotransmission and development. *Journal of Anatomy*, *224*(1), 61–73. https://doi.org/10.1111/joa.12106.

Martin, P. T., & Sanes, J. R. (1997). Integrins mediate adhesion to agrin and modulate agrin signaling. *Development*, *124*(19), 3909–3917.

McClure, M. J., Clark, N. M., Hyzy, S. L., Chalfant, C. E., Olivares-Navarrete, R., Boyan, B. D., & Schwartz, Z. (2016). Role of integrin α7β1 signaling in myoblast differentiation on aligned polydioxanone scaffolds. *Acta Biomaterialia*, *39*, 44–54. https://doi.org/10.1016/j.actbio.2016.04.046.

Menon, K. P., Carrillo, R. A., & Zinn, K. (2013). Development and plasticity of the *Drosophila* larval neuromuscular junction. *Wiley Interdisciplinary Reviews: Developmental Biology*, *2*(5), 647–670.

Piette, J., Bessereau, J.-L., Huchet, M., & Changeux, J.-P. (1990). Two adjacent MyoD1-binding sites regulate expression of the acetylcholine receptor (alpha)-subunit gene. *Nature*, *345*(6273), 353–355.

Ricotti, L., Polini, A., Genchi, G. G., Ciofani, G., Iandolo, D., Vazão, H., … Pisignano, D. (2012). Proliferation and skeletal myotube formation capability of C2C12 and H9c2 cells on isotropic and anisotropic electrospun nanofibrous PHB scaffolds. *Biomedical Materials*, *7*(3), 035010.

Rudnicki, M. A., & Jaenisch, R. (1995). The MyoD family of transcription factors and skeletal myogenesis. *BioEssays*, *17*(3), 203–209. https://doi.org/10.1002/bies.950170306.

Shrirao, A. B., Kung, F. H., Yip, D., Cho, C. H., & Townes-Anderson, E. (2014). Vacuum-assisted fluid flow in microchannels to pattern substrates and cells. *Biofabrication*, *6*(3), 035016.

Shrirao, A. B., Kung, F. H., Yip, D., Firestein, B. L., Cheul, H., & Townes-Anderson, E. (2017). A versatile method of patterning proteins and cells. *JoVE (Journal of Visualized Experiments)*, *120*, e55513.

Smith, C. L., Mittaud, P., Prescott, E. D., Fuhrer, C., & Burden, S. J. (2001). Src, Fyn, and Yes are not required for neuromuscular synapse formation but are necessary for stabilization of agrin-induced clusters of acetylcholine receptors. *The Journal of Neuroscience*, *21*(9), 3151–3160.

Sokolov, P. A., Belousov, M. V., Bondarev, S. A., Zhouravleva, G. A., & Kasyanenko, N. A. (2017). FibrilJ: ImageJ plugin for fibrils' diameter and persistence length determination. *Computer Physics Communications*, *214*, 199–206. https://doi.org/10.1016/j.cpc.2017.01.011.

Tintignac, L. A., Brenner, H.-R., & Rüegg, M. A. (2015). Mechanisms regulating neuromuscular junction development and function and causes of muscle wasting. *Physiological Reviews*, *95*(3), 809–852.

Tourovskaia, A., Kosar, T. F., & Folch, A. (2006). Local induction of acetylcholine receptor clustering in myotube cultures using microfluidic application of agrin. *Biophysical Journal*, *90*(6), 2192–2198. https://doi.org/10.1529/biophysj.105.074864.

Tourovskaia, A., Li, N., & Folch, A. (2008). Localized acetylcholine receptor clustering dynamics in response to microfluidic focal stimulation with agrin. *Biophysical Journal*, *95*(6), 3009–3016.

Trinidad, J. C., Fischbach, G. D., & Cohen, J. B. (2000). The agrin/MuSK signaling pathway is spatially segregated from the neuregulin/ErbB receptor signaling pathway at the neuromuscular junction. *Journal of Neuroscience*, *20*(23), 8762–8770.

Weintraub, H. (1993). The MyoD family and myogenesis: Redundancy, networks, and thresholds. *Cell*, *75*(7), 1241–1244. https://doi.org/10.1016/0092-8674(93)90610-3.

Weston, C. A., Teressa, G., Weeks, B. S., & Prives, J. (2007). Agrin and laminin induce acetylcholine receptor clustering by convergent, Rho GTPase-dependent signaling pathways. *Journal of Cell Science*, *120*(5), 868–875. https://doi.org/10.1242/jcs.03367.

Whitehead, T. J., & Sundararaghavan, H. G. (2014). Electrospinning growth factor releasing microspheres into fibrous scaffolds. *Journal of Visualized Experiments*, *90*. https://doi.org/10.3791/51517.

Yang, H. S., Ieronimakis, N., Tsui, J. H., Kim, H. N., Suh, K.-Y., Reyes, M., & Kim, D.-H. (2014). Nanopatterned muscle cell patches for enhanced myogenesis and dystrophin expression in a mouse model of muscular dystrophy. *Biomaterials*, *35*(5), 1478–1486. https://doi.org/10.1016/j.biomaterials.2013.10.067.

Zhang, D., Sun, M. B., Lee, J., Abdeen, A. A., & Kilian, K. A. (2016). Cell shape and the presentation of adhesion ligands guide smooth muscle myogenesis. *Journal of Biomedical Materials Research Part A*, *104*(5), 1212–1220. https://doi.org/10.1002/jbm.a.35661.

How to cite this article: Kung FH, Sillitti D, Shrirao AB, Shreiber DI, Firestein BL. Collagen nanofibre anisotropy induces myotube differentiation and acetylcholine receptor clustering. *J Tissue Eng Regen Med*. 2018;12:e2010–e2019. https://doi.org/10.1002/term.2632